14. Argyle, E. *Icarus* **77,** 220–222 (1989).
15. O'Keefe, J. D. & Ahrens, T. J. in *Geological Implications of Impacts of Large Asteroids and Comets on the Earth, Geol. Soc. Am. Spec. Pap.* 190, 103–120 (1982).
16. Melosh, H. J. in *Geological Implications of Impacts of Large Asteroids and Comets on the Earth, Geol. Soc. Am. Spec. Pap.* 190, 121–127 (1982).
17. Kyte, F. T., Smit, J. & Wasson, J. T. *Earth planet. Sci. Lett.* **73,** 183–195 (1985).
18. Bohor, B. F., Triplehorn, D. M., Nichols, D. J. & Millard, H. T. J. *Geology* **15,** 896–899 (1987).
19. Glasstone, S. & Dolan, P. J. *Effects of Nuclear Weapons* Table 7.40 (US Departments of Defense and Energy, Washington, DC, 1977).
20. Bate, R. D., Mueller, D. D. & White, J. E. *Fundamentals of Astrodynamics* (Dover, New York, 1971).
21. Whipple, F. L. *Proc. Natn. Acad. Sci. U.S.A.* **36,** 687–695 (1950).
22. Brownlee, D. E. *A. Rev. Earth planet. Sci.* **13,** 147–173 (1985).
23. Chamberlain, J. W. & Hunten, D. M. *Theory of Planetary Atmospheres* 1–481 (Academic, Orlando, 1987).
24. Zahnle, K. J. in *Global Catastrophes, Geol. Soc. Am. Spec. Pap.* (in the press).
25. LaRocca, A. L. in *The Infrared Handbook* (eds Wolfe, W. L. & Zissis, G. J.) 5.1–5.132 (Office of Naval Research, Alexandria, Virginia 1978).
26. Holton, J. R. *Introduction to Dynamic Meteorology* 2nd edn, 1–391 (Academic, New York, 1979).
27. Hildebrand, A. R. & Wolbach, W. S. *Lunar planet. Sci. Conf. XX* (abstr.) 414–415 (1989).
28. Martin, S. *Proc. 10th Symp. (Int.) on Combustion* 877–896 (Williams and Wilkins, Baltimore, 1965).
29. Simms, D. L. & Law, M. *Combust. Flame* **11,** 377–388 (1967).
30. Simms, D. L. *Combust. Flame* **7,** 253–261 (1963).
31. Argyle, E. *Science* **234,** 261 (1986).

ACKNOWLEDGEMENTS. We thank A. Hildebrand for discussion of the K/T boundary-layer thickness and petrology, D. Grinspoon for discussion early in this study, R. Selkirk for information on clouds and G. Shoemaker for comments.

Evidence from carbon isotope measurements for diverse origins of sedimentary hydrocarbons

Katherine H. Freeman*, J. M. Hayes*, Jean-Michel Trendel† & Pierre Albrecht†

* Biogeochemical Laboratories, Departments of Chemistry and of Geology, Geology Building, Indiana University, Bloomington, Indiana 47405-5101, USA
† Laboratoire de Chimie Organique des Substances Naturelles, Département de Chimie, Université Louis Pasteur, 1 rue Blaise Pascal, 67008 Strasbourg, France

THE organic matter found in sedimentary rocks must derive from many sources; not only from ancient primary producers but also from consumers and secondary producers. In all of these organisms, isotope effects can affect the abundance and distribution of ^{13}C in metabolites. Here, by using an improved form of a previously described technique[1] in which the effluent of a gas chromatograph is continuously analysed isotopically, we report evidence of the diverse origins of sedimentary organic matter. The record of ^{13}C abundances in sedimentary carbonate and total organic carbon can be interpreted in terms of variations in the global carbon cycle (see ref. 2, for example) Our results demonstrate, however, that isotope variations within sedimentary organic mixtures substantially exceed those observed between samples of total organic carbon[3]. Resolution of isotope variations at the molecular level offers a new and convenient means of refining views both of localized palaeoenvironments and of control mechanisms within the global carbon cycle.

We summarize the carbon isotopic compositions of individual branched and cyclic hydrocarbons extracted[4] from the Eocene Messel Shale in Table 1. These values were obtained by integrating the mass 44, 45 and 46 ion currents from the carbon dioxide produced by continuous combustion of the chromatographic effluent (Fig. 1). The performance of this technique is limited by the chromatographic resolution, the accuracy of calibration of the scale of isotope abundances (δ-values) and the adequacy of corrections for background carbon dioxide (largely derived from combustion of column bleed). Because well developed procedures for deconvoluting the contributions of unresolved components are not yet available, there are systematic errors in δ-values if contributions from co-eluting substances are significant. As shown in Fig. 2, such contributions lead to recognizable fluctuations in the 45/44 ion current ratio. Peaks for which there is evidence of co-eluting components are indicated in Table 1 and discussed below.

We refer the isotopic compositions to the PDB ^{13}C standard by comparison to co-injected standards; it is particularly important that these standards be well resolved. Here, the worst case is that of the standard following peak 19. Multiple analyses under varying conditions are represented by the extremes shown by Figs 1 and 2. In Fig. 2, the width of the standard peak at 10% of peak height is 21 s. Measured from baseline to baseline, the width of the corresponding oscillation in the ratio plot is 26 s. The approximately flat interval between the major oscillations in the ratio plot marks a clear separation of the isotope signals and is 25 s in width. A slightly overloaded chromatogram is shown in Fig. 1 because the large quantity of sample injected provides a clear view of minor peaks. In the corresponding ratio plot, the oscillation associated with the standard peak is 22 s in width and there is a flat interval of 10 s between the peaks. When limits of integration are selected to exclude minor components and background corrections are based on a line placed by interpolation between peak-free intervals in the chromatograms, the δ-values for peak 19 are $-21.2‰$ for data shown in Fig. 2 and $-21.2‰$ for the data shown in Fig. 1. Eight different determinations of the δ-value for peak 19 range from -19.6 to $-21.5‰$ and average $-20.9‰$. The standard deviation of the population is 0.6‰ and, on that basis, the 95% confidence limits are estimated at 0.5‰ (s.e.m. = 0.2‰, $t = 2.36$).

In a previous study of this unit, isotope analyses were performed on bulk phases (such as crude fractions of extracts) and a few compounds laboriously isolated using preparative techniques[5]. This work established carbon isotopic compositions of some Messel primary producers (eukaryotic algae, $-22‰$; green photosynthetic bacteria, $-24‰$) and of lipids produced by dinoflagellates in the lake's aerobic photic zone ($-25‰$) and by methanogenic bacteria in anaerobic portions of the water column or sediments ($-30‰$). It was suggested that, in Lake Messel, methane rising from anaerobic zones must have been used as a carbon source by aerobic methanotrophs. Methane produced by fermentative processes in lake sediments is commonly depleted in ^{13}C (ref. 6). The appearance in Table 1 of abundant compounds strongly depleted in ^{13}C (peaks 8, 10, 11, 15, discussed below) confirms the hypothesis of methane recycling. Other features of the isotope distribution reflect the carbon pathways in, and therefore the details of, this ancient environment. Together with a recent study of functionalized lipids from the Messel Shale[7], our results offer a perspective on Messel biogeochemistry that is different from the one provided by a recent chemical and morphological examination of Messel Shale kerogen, which indicated that the organic matter derived primarily from a single algal species[8].

Pristane and phytane (peaks 3 and 4, Table 1) are acyclic isoprenoid biomarkers of broad geochemical interest. Their derivation has been commonly discussed in terms of oxidation or

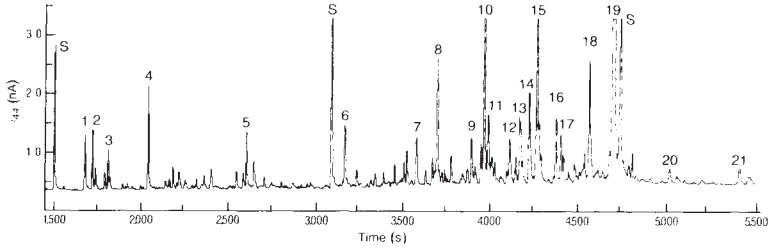

FIG. 1 Branched and cyclic alkanes extracted from the Messel Shale. Mass-44 ion current as a function of time for continuous combustion of chromatographic effluent (1-V signal corresponds to 3.3-nA ion current). Peaks are numbered as in Table 1 (S marks standard peaks). Column: 30 m × 0.32-mm inner diameter methyl silicone (Ultra-1); temperature program was 60–320 °C at 3° min^{-1}, then isothermal at 320 °C for 30 min.

TABLE 1 Carbon isotopic compositions of individual compounds

Peak	t_R* (s)	Amount† (nmol C)	$\delta^{13}C$‡ (‰)	Identification
1	1,679	1.1	−22.7 ± 1.0	norpristane
2	1,722	1.0	−30.2 ± 0.3	C_{19} acyclic isoprenoid
3	1,812	0.7	−25.4 ± 1.0	pristane
4	2,040	2.0	−31.8 ± 0.8	phytane
5	2,602	1.0	−29.1 ± 0.6	C_{23} acyclic isoprenoid
6	3,161	1.3	−23.9 ± 0.6	10β(H)-des-*A*-lupane
7	3,571	1.3	−24.9 ± 1.0	mixture of hydrocarbons
8	3,688	2.6	−73.4 ± 1.3	C_{32} acyclic isoprenoid
9	3,883	0.9	−24.2 ± 1.2	isoprenoid alkane
10	3,957	6.8	−49.9 ± 1.1	17β(H)-22,29,30-trisnorhopane
11	3,977	2.0	−60.4 ± 1.8	isoprenoid alkane
12	4,100	1.6	−43.5 ± 1.0	17α(H),21β(H)-30-norhopane
13	4,156	2.0	~ −45	17β(H),21α(H)-30-norhopane§
14	4,210	2.9	~ −34	17α(H),21β(H)-hopane‖
15	4,256	6.2	−65.3 ± 1.4	17β(H),21β(H)-30-norhopane
16	4,364	1.8	−39.4 ± 0.8	17α(H),21β(H)-homohopane
17	4,392	1.3	−35.2 ± 1.4	17β(H),21β(H)-hopane
18	4,552	4.2	−36.6 ± 0.5	17β(H),21β(H)-homohopane
19	4,692	15.4	−20.9 ± 0.5	lycopane¶
20	5,010	0.5	−27.0 ± 0.4	unknown hydrocarbon
21	5,408	0.8	−28.8 ± 1.0	unknown hydrocarbon

* Chromatographic retention time (Fig. 1).

† Amounts of carbon represented by peaks in Fig. 1.

‡ $\delta = 10^3[(R_x - R_s)/R_s]$, where $R = {}^{13}C/{}^{12}C$, x designates sample, s designates PDB standard and $R_s = 0.0112372$. Entries are mean and 95% confidence interval for two to eight replicate measurements.

§ Peak contains another component, apparently an isoprenoid alkane ($\delta \sim -22$‰).

‖ Peak contains another component, probably a C_{30} 4-methyl sterane. By contrast with the situation in peak 13, variations in the ratio plot indicate that δ values of the unresolved components do not differ by more than 10‰.

¶ Peak also contains minor component, apparently an acyclic isoprenoid.

reduction of phytol[9], although the possibility of alternate origins is recognized[10]. Here, their isotopic compositions differ significantly and require separate origins. The δ-value for pristane fits with that expected for algal lipids (−25‰). That of phytane is 5‰ lower, but does not differ significantly from that previously observed for ether-linked polyisoprenoids in these sediments (−29.8‰, ref. 5). Together with results of stereochemical investigations[11], these observations strongly suggest derivation of phytane principally from lipids of methanogenic bacteria. The C_{19} acyclic isoprenoid in peak 2 and the C_{23} acyclic isoprenoid (peak 5) probably share this source. The 10β(H)-des-*A*-lupane[12,13] may derive from photochemical or bacterial photomimetic decomposition of pentacyclic triterpenoids from higher plants[12], and thus may record their isotopic composition. The δ-value exceeds that previously observed for leaf material from Eocene land plants (−27.5‰) and for isoarborinol (−28.1‰) isolated from the Messel Shale[5]. It is possible: (1) that both isoarborinol and the lupane are of higher-plant origin, the latter deriving from ^{13}C-enriched aquatic macrophytes[14] and the former from land plants, or (2) that the lupane is representative of terrestrial plants that were, like some modern tropical plants, relatively enriched in ^{13}C (ref. 3). In the latter case, as previously suggested[15], a microbial origin is likely for isoarborinol. Norpristane (peak 1), the compound in peak 9, and possibly lycopane, may all have the same source as the des-*A*-lupane. Other compounds possibly related to primary producers are the late-eluting peaks 20 and 21, which have isotopic compositions consistent with a terrestrial-plant origin.

Although its structure is not known in detail, the isotopic composition of the C_{32} acyclic polyisoprenoid in peak 8 indicates that it was derived from methanotrophic bacteria. A normal kinetic isotope effect of up to 25‰ is associated with the assimilation of methane by these organisms[16], which will, therefore, be even more strongly depleted in ^{13}C than their carbon source. The extent of depletion depends on the efficiency with which the bacteria are able to capture the methane. In a natural, open system, that efficiency is likely to have been low, and peak 8 may be as much as 25‰ depleted in ^{13}C relative to the methane. Therefore, we now estimate $-48 \geq \delta(CH_4) \geq -73$‰ in Lake Messel, in excellent agreement with observations of $\delta(CH_4)$ in modern lacustrine systems[6].

Other compounds so strongly depleted in ^{13}C that they are probably derived, at least in part, from methanotrophs are the C_{29} hopane[4,17] in peak 15, the C_{27} hopane[4,17] in peak 10 and the acyclic polyisoprenoid in peak 11. As polyisoprenoids, these would derive from the same biosynthetic pathway as the compound in peak 8. Had they been synthesized by the same organism, they would have the same isotopic composition. The significant enrichment in ^{13}C relative to peak 8 indicates either an origin from a different methanotroph or, more likely, partial derivation from nonmethanotrophic sources. This is particularly clear in the case of 17β(H),21β(H)-30-norhopane (peak 15), which is the most likely degradation product (by oxidation and decarboxylation)[18] of the C_{35} aminopentol that is the most abundant hopanoid in *Methylococcus capsulatus* and in *Methylomonas sp.*[18,19]. This same C_{29} hopane is a common constituent of many sediments that do not bear similar evidence of methanotrophy[17,20], and can derive from a variety of bacterial sources[20,21].

The ubiquitous bacterial hopanes comprise the remaining entries in Table 1. Notably, these include the αβ- and βα-stereoisomers[22] of the ^{13}C-depleted ββ-C_{29}-hopane in peak 15.

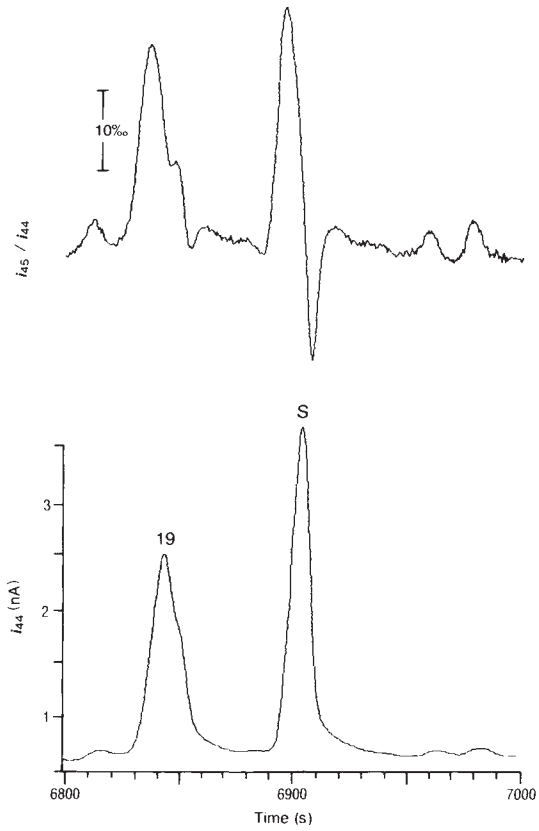

FIG. 2 The lower plot is an expanded view of the region around peak 19 in a chromatogram of the same sample shown in Fig. 1. In this case, the total sample load was fourfold lower and the rate of the temperature programme was 2° min^{-1}. Retention times were longer and peaks were wider, but resolution improved. The upper plot shows the mass-45/mass-44 ion current ratio. Because alkanes containing one or more ^{13}C atoms migrate through the chromatographic system more rapidly than those containing only ^{12}C, $^{13}CO_2$ (mass 45) precedes $^{12}CO_2$ (mass 44) at the ion source. For the standard peak shown here (S), this causes the ratio signal first to increase sharply, indicating that the leading edge of the standard peak is enriched in ^{13}C relative to the background, then drop to values below the baseline as the later, ^{12}C-rich portion of the peak is eluted. Because peak 19 is relatively enriched in ^{13}C, the negative portion of its ratio oscillation is small. The appearance of an extra inflection in the ratio plot for peak 19 indicates the presence of more than one component or, possibly, a mixture of diastereomers.

Isotope differences indicate that the αβ- and βα-isomers cannot have derived from epimerization of average ββ-C_{29}-hopane. Through its mechanism or environment[23–26], the process of epimerization must have operated selectively on a precursor pool that happened to be isotopically distinct. Isotopic compositions of the remaining hopanes range from −34 to −39‰. Although even this variation may reflect minor methanotrophic inputs, it is more useful to consider these materials as end-members. What organisms might have produced them and how might their isotopic compositions be explained? One clue is furnished by the isotopic composition of nitrogen in Messel kerogen. Analysis yields $\delta^{15}N = +6.8$‰ relative to air (J. W. Collister, personal communication). This ^{15}N enrichment indicates active recycling of nitrogen, probably involving ammonia-oxidizing bacteria[27]. Such organisms are microaerophilic chemoautotrophs known to synthesize hopanoids[21]. In Lake Messel, these bacteria would have grown at the oxycline and used dissolved carbon dioxide as their carbon source ($\delta \sim -14$‰, estimated from isotopic composition of green photosynthetic bacteria and from the isotope effect associated with carbon fixation[28,29]). Ammonia-oxidizing bacteria use the C_3 pathway of carbon fixation. Depending on the concentration of dissolved carbon dioxide, they will be depleted in ^{13}C relative to their carbon source by up to 27‰ (ref. 30). Depletions of ~20‰ are plausible and would yield δ(whole organisms) = −34‰, δ(hopanoids) ≈ −37‰. Chemoautotrophic bacteria are, thus, a possible source of biomarker lipids depleted in ^{13}C relative to total organic carbon (a similar situation will arise in marine sediments if, as is likely, sulphide-oxidizing bacteria[31] use ^{13}C-depleted carbon dioxide at the base of the aerobic zone).

We cannot exclude heterotrophic bacteria as a source for the ^{13}C-depleted hopanes. Bacterial reworking of primary biological inputs must have been particularly important in anaerobic portions of the water column and in the sediments, in which a fermentative community produced considerable quantities of methane. Unfortunately, little is known regarding intermolecular isotopic fractionations within such communities. In an environment in which δ-values of fresh biological material ranged from −20 to −75‰, almost any composition might be found, particularly if seasonal factors affected sources of organic material. Moreover, a compound with $\delta = -55$‰ might derive, not from a 1:1 mixture of −35 and −75‰ endmembers, but from synthesis by an organism that used both ^{13}C-rich and ^{13}C-poor carbon sources.

Although uncertainties in isotope ratios would be decreased if we used preliminary chromatographic steps to prepare simpler mixtures, the isotopic differences evident in Table 1 demonstrate the value of molecular isotope analyses for the study of natural systems. From the viewpoint of biogeochemistry, it seems that sedimentary organic compounds must increasingly be viewed as products of a microbial community, not merely as residues of primary production. □

Received 3 July; accepted 21 November 1989.

1. Matthews, D. E. & Hayes, J. M. *Analyt. Chem.* **50,** 1465–1473 (1978).
2. Knoll, A. H., Hayes, J. M., Kaufman, A. J., Swett, K. & Lambert, I. B. *Nature* **321,** 832–838 (1986).
3. Deines, P. in *Handbook of Environmental Isotope Geochemistry* Vol. 1A (eds Fritz, P. & Fontes, J. C.) 329–406 (Elsevier, Amsterdam, 1980).
4. Kimble, B. J. *et al. Geochim. cosmochim. Acta* **38,** 1165–1181 (1974).
5. Hayes, J. M., Takigiku, R., Ocampo, R., Callot, H. J. & Albrecht, P. *Nature* **329,** 48–51 (1987).
6. Whiticar, M. J., Faber, E. & Schoell, M. *Geochim. cosmochim. Acta* **50,** 693–709 (1986).
7. Robinson, N., Eglinton, G., Cranwell, P. A. & Zeng, Y. B. *Chem. Geol.* **76,** 153–173 (1989).
8. Goth, K., deLeeuw, J. W., Puttmann, W. & Tegelaar, E. W. *Nature* **336,** 759–761 (1988).
9. Didyk, B. M., Simoneit, B. R. T., Brassell, S. C. & Eglinton, G. *Nature* **272,** 216–222 (1978).
10. ten Haven, H. L., deLeeuw, J. W., Rullkotter, J. & Sinninghe Damste, J. S. *Nature* **330,** 641–643 (1987).
11. Risatti, J. B., Rowland, S. J., Yon, D. A. & Maxwell, J. R. *Org. Geochem.* **6,** 93–104 (1984).
12. Corbet, B., Albrecht, P. & Ourisson, G. *J. Am. chem. Soc.* **192,** 1171–1173 (1980).
13. Trendel, J-M. *et al. Tetrahedron* **45,** 4457–4470 (1989).
14. Osmond, C. B., Valaane, N., Haslam, S. M., Uotila, P. & Roksandic, Z. *Oecologia* **50,** 117–124 (1981).
15. Ourisson, G., Albrecht, P. & Rohmer, M. *Trends Biochem. Sci.* **7,** 236–239 (1982).
16. Coleman, D. D., Risatti, J. B. & Schoell, M. *Geochim. cosmochim. Acta* **45,** 1033–1037 (1981).
17. Ensminger, A., Van Dorsselaer, A., Spyckerelle, Ch., Albrecht, P. & Ourisson, G. in *Advances in Organic Geochemistry 1973* (eds Tissot, B. P. & Bienner, F.) 245–260 (Technip, Paris, 1973).
18. Zundel, M. & Rohmer, M. *FEMS Microbiol. Lett.* **28,** 61–64 (1985).
19. Neunlist, S. & Rohmer, M. *Biochem. J.* **231,** 635–639 (1985).
20. Ourisson, G., Rohmer, M. & Albrecht, P. *Pure appl. Chem* **51,** 709–729 (1979).
21. Ourisson, G., Rohmer, M. & Poralla, K. *A. Rev. Microbiol.* **41,** 301–333 (1987).
22. Van Dorsselaer, A., Albrecht, P. & Ourisson, G. *Bull. Soc. chim. Fr.* 165–170 (1977).
23. Quirke, J. M., Wardroper, A. M. K., Wheatley, R. E. & Maxwell, J. R. *Chem. Geol.* **42,** 25–43 (1984).
24. Michaelis, W., Richnow, H. H. & Jenisch, A. *Sci. Total Envir.* **81/82,** 41–50 (1989).
25. Seifert, W. K. & Moldowan, J. M. in *Advances in Organic Geochemistry 1979* (eds Douglas, A. G. & Maxwell, J. R.) 229–237 (Pergamon, Oxford, 1980).
26. Ries-Kautt, M. & Albrecht, P. *Chem. Geol.* **76,** 143–151 (1989).
27. Collister, J. W., & Hayes, J. M. *Bull. U.S. geol. Surv.* (in the press).
28. Sirevag, R., Buchanan, B. B., Berry, J. A. & Troughton, J. H. *Arch. Microbiol.* **112,** 35–38 (1977).
29. Fry, B. *Limnol. Oceanogr.* **31,** 79–88 (1986).
30. Popp, B. N., Takigiku, R., Hayes, J. M., Louda, J. W. & Baker, E. W. *Am. J. Sci.* **289,** 436–454 (1989).
31. Kepkay, P. E., Cooke, R. C. & Novitsky, J. A. *Science* **204,** 68–69 (1979).

ACKNOWLEDGEMENTS. We thank S. A. Studley for technical assistance, M. P. Ricci for development of isotope-ratio-monitoring software, and M. Rohmer and J. W. Collister for discussions. We also thank NASA, Chevron Oil Field Research Corporation and Finnigan MAT for support.

Magnetic iron-sulphur crystals from a magnetotactic microorganism

Marcos Farina*, Darci Motta S. Esquivel† & Henrique G. P. Lins de Barros†‡

* Insituto de Biofisica, UFRJ, Cidade Universitaria, Ilha do Fundao, Rio de Janeiro 21941, Brazil
† Centro Brasileiro de Pesquisas Fisicas, CBPF/CNPq, Rua Xavier Sigaud 150, 22290 Urca, Rio de Janeiro, Brazil

IN all magnetotactic microorganisms studied so far, the geomagnetic field is detected by magnetic particles with a permanent magnetic moment. These are crystallites enveloped by a membrane that forms the magnetosome, a specialized organelle common to magnetotactic cells[1,2]. To date, the magnetic crystallite of magnetotactic bacteria has been found to be magnetite, an iron-oxygen mineral[3–7]. Here we report the discovery of magnetic iron-sulphur crystals in a highly motile multicellular aggregate of bacteria found in brackish water with sulphide-rich sediments. The iron sulphide crystals are enveloped by amorphous or weakly crystalline regions rich in iron and oxygen, and these regions are surrounded by a membrane forming the magnetosome. The oxygen-rich region may be involved in growth of the iron sulphide crystals. The magnetosomes are found in planar groups inside the cytoplasm of each cell in the aggregate. Magnetic iron sulphide such as we describe here, which is probably pyrrhotite, may be a source of remnant magnetization in sediments and soils.

We have studied sediments from marine lakes at latitudes between 7° and 27° in the Southern Hemisphere; as well as coccus bacteria we found a highly motile flagellar magnetotactic multicellular aggregate (MMA) of diameter between 5 and 10 μm, which orientates in the geomagnetic field. The typical magnetic moment is 10^{-11} e.m.u. These organisms are composed of about twenty double individual cells bounded by two membranes, and they contain more than 1,000 crystals that are not completely orientated. MMAs were collected at depths varying from ~20 cm to >1 m in marine or brackish water at the interface between water and sediment. Their fine-structure and behavioural response have been described[8].

Differential interference contrast optical microscopy and scanning electron microscopy (SEM) show that each aggregate is made up of cells morphologically arranged in a helicoidal-like distribution. In low-salinity medium (distilled water added to the sample), living organisms disaggregate into individual components that have neither magnetic orientation nor movement. Living individual components have never been observed. SEM and transmission electron microscopy (TEM) were used in conjunction with fixation techniques previously described[9].

‡ To whom correspondence should be addressed.